Special Issue Article

Advances in Mechanical Engineering

Advances in Mechanical Engineering
2017, Vol. 9(12) 1–10
© The Author(s) 2017
DOI: 10.1177/1687814017739513
journals.sagepub.com/home/ade
SAGE

Structural analysis and optimization of bicycle frame designs

Chien-Cheng Lin[1,2], Song-Jeng Huang[1] and Chi-Chia Liu[3]

Abstract

This article analyzes the stress and optimizes the design of a customized bicycle frame using Pro/ENGINEER digital solid modeling computer-aided design software. This study attempts to verify the stress and displacement response of several types of bicycle frames using a wireframe model and then analyze the solid structure. In summary, for a shell-entity frame, the diamond-type frame (diamond-shaped) has the highest rigidity. The mechanical properties of AZ60/Al_2O_{3p} magnesium metal matrix nanocomposites by equal channel angular extrusion almost achieve the level of Al6061 aluminum.

Keywords

Bicycle frame, computer-aided engineering, equal channel angular extrusion, optimized design, sensitivity analysis

Date received: 31 May 2017; accepted: 5 October 2017

Handling Editor: Stephen D Prior

Introduction

As bicycles are environmentally friendly, safe and are a form of exercise with many other advantages, the government of Taiwan and the bicycle industry have promoting them as green products. Taiwan is a major producer of bicycles and their components and is a center for the development of manufacturing process technology and materials science. The appearance of a bicycle is no longer limited to the traditional style; research and development have led to ergonomic designs with low-riding drag, a lightweight frame, greater strength, and improved handling to meet customized needs.[1] There are several challenges faced during the integration of customer/user requirements into the design process.[2,3] In many instances, customers do not have knowledge on how to design the product, and customer-specified configurations need to be feasible and optimized for performance.

Schuijbroek et al.[4] designed optimal vehicle routes to rebalance the inventory. The purpose of this research is to analyze the stress on bicycle frames and optimize their design using Pro/ENGINEER software to establish numerical simulations. The bicycle frame is a standard component of a bicycle, and every bicycle factory has a different design. Other important components are the tires, wheels, and pedals. The geometry of the frame governs the properties and performance of the bicycle. The lengths and angles of the frame affect a rider's riding comfort and behavior.[5,6]

This article analyzes the stress and optimizes the design of a customized bicycle frame using Pro/

[1]Composites and Solid Mechanics Lab, Department of Mechanical Engineering, National Taiwan University of Science and Technology, Taipei, Taiwan, R.O.C.
[2]Opto-Mechatronics Technology Center, Department of Mechanical Engineering, National Taiwan University of Science and Technology, Taipei, Taiwan, R.O.C.
[3]Department of Industrial Education, National Taiwan Normal University, Taipei, Taiwan, R.O.C.

Corresponding author:
Chien-Cheng Lin, Opto-Mechatronics Technology Center, Department of Mechanical Engineering, National Taiwan University of Science and Technology, No. 43, Keelung Road, Sec. 4, Taipei 10607, Taiwan, R.O.C.
Email: d10003206@mail.ntust.edu.tw

ENGINEER digital solid modeling and design software, through high-resolution numerical computer-aided engineering (CAE) simulations of bicycle frame, stress analysis, numerical analysis, and optimal designs of the frame structure. As the motor vehicle is still the main form of domestic private transport, there has been no consideration of the environmental impact of customized bicycle frames. At present, many scholars and institutions have undertaken the research of personalized bicycle design and got some achievements. For instance, XJ Liu et al.[7] founded optimum solutions to get suitable seat height and crank length for a person are obtained accordingly. Also this research is of significance for customizing bicycles and design of bicycle robot.

Essential issues

In recent years, due to the excessive exploitation and rising use of petroleum for energy, modern industry, and transportation are contributing toward emission of exhaust gases, such as carbon dioxide, causing global warming. Global warming causes the melting of polar icecaps, leading to rising sea levels and the disappearance of land. Many scientists and environmental groups are committed to the development of new technology to solve the hazards and environmental issues arising from old technology. However, new technologies inevitably lead to new environmental problems. Figure 1 shows the main structure of a bicycle frame. In accordance with its functions, a bicycle structure can be divided into five parts: body (skeleton), steering system, braking systems, wheel system, and the transmission system.[8] In this article, the research focused on bicycle frames. The other components lie outside the scope of the research.

This study designs and establishes a standard analysis procedure for bicycle frames because multiple analyses are often performed on a single component, as shown in Figure 2. Using Pro/MECHANICA CAE software as a research tool, computer simulations and analysis were performed. In addition, to simplify file management, this article establishes a design procedure, and all analyses are added to this procedure.

In this article, we used the lightweight and new materials to improve the structural rigidity and energy-saving of riding. Therefore, Al6061 aluminum alloy, AZ61 magnesium alloy, and AZ61/Al_2O_{3p} magnesium metal matrix nanocomposites (MMC) were processed using equal channel angular extrusion (ECAE),[9,10] to make it more innovative and to enhance superior strength as compared to other bicycle frame materials.

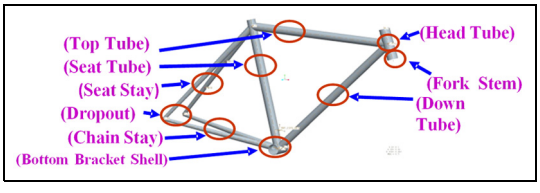

Figure 1. Main structure of a bicycle frame.

Numerical method

Structural analysis of frame with Pro/ENGINEER digital solid modeling

Using the finite element method (FEM), we consider a frame experiencing a force P. We also derive the stiffness coefficient and the equation of the center load, as shown in Figure 3(a) and equation (1)

$$\{U\} = \{T\}\{u\}$$

$$\{U\} = \begin{Bmatrix} U_{iX} \\ U_{iY} \\ U_{jX} \\ U_{iY} \end{Bmatrix}, [T] = \begin{bmatrix} \cos\theta & -\sin\theta & 0 & 0 \\ \sin\theta & \cos\theta & 0 & 0 \\ 0 & 0 & \cos\theta & -\sin\theta \\ 0 & 0 & \sin\theta & \cos\theta \end{bmatrix} \quad (1)$$

The local and global displacements and force coordinates are shown in Figure 3(a), and equation (2) represents the displacement of nodes i and j in the global X–Y and local x–y reference coordinates, where T is the transformation matrix, with the local deformation transferred into the individual's global value[11]

$$\{u\} = \begin{Bmatrix} u_{ix} \\ u_{iy} \\ u_{jx} \\ u_{jy} \end{Bmatrix} \quad (2)$$

Based on equation (2), the local coordinates are related to the global force. The general form of the matrix can be expressed as

$$[T]^{-1}\{P\} = [K][T]^{-1}\{p\} \quad (3)$$

where $[T]^{-1}$ is the inverse of the transformation matrix [T], calculated as follows. We multiply both sides of equation (1) with [T] and simplify to obtain the following expression by substituting the values of $[T]$, $[K]$, $[T]^{-1}$ into equation (1) and multiply by {U}

$$\{P\} = [T][K][T]^{-1}\{U\} \quad (4)$$

The relationship between the deflection of the load, the element stiffness matrix, $[K]^{(e)}$, and any global element node is given by

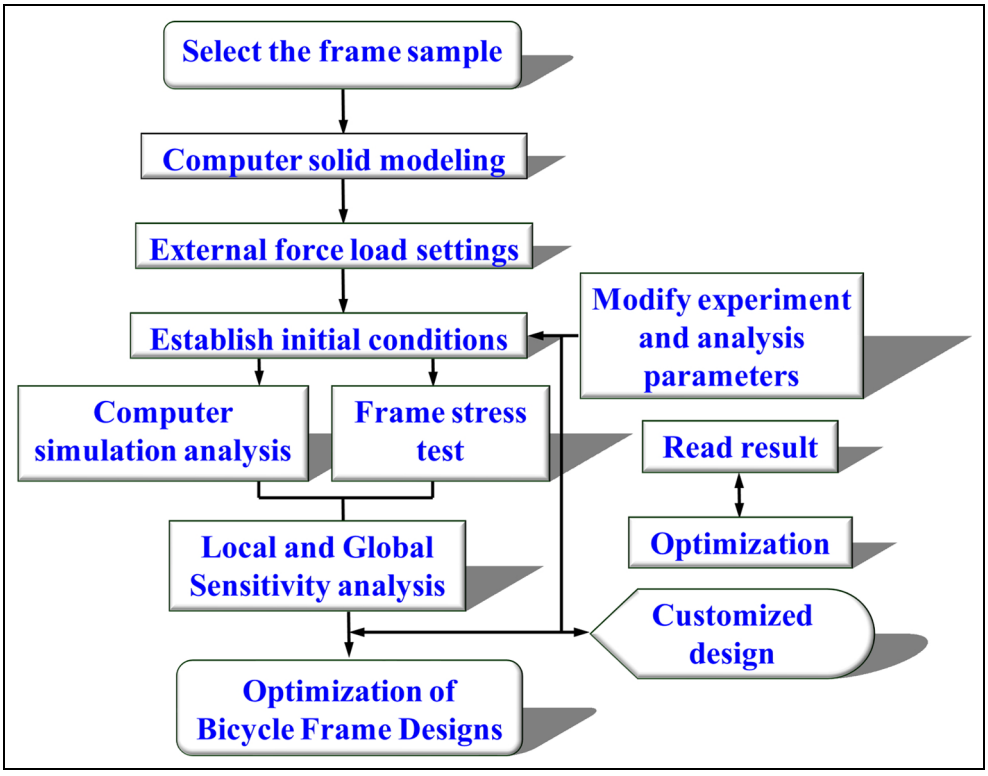

Figure 2. Research procedures.

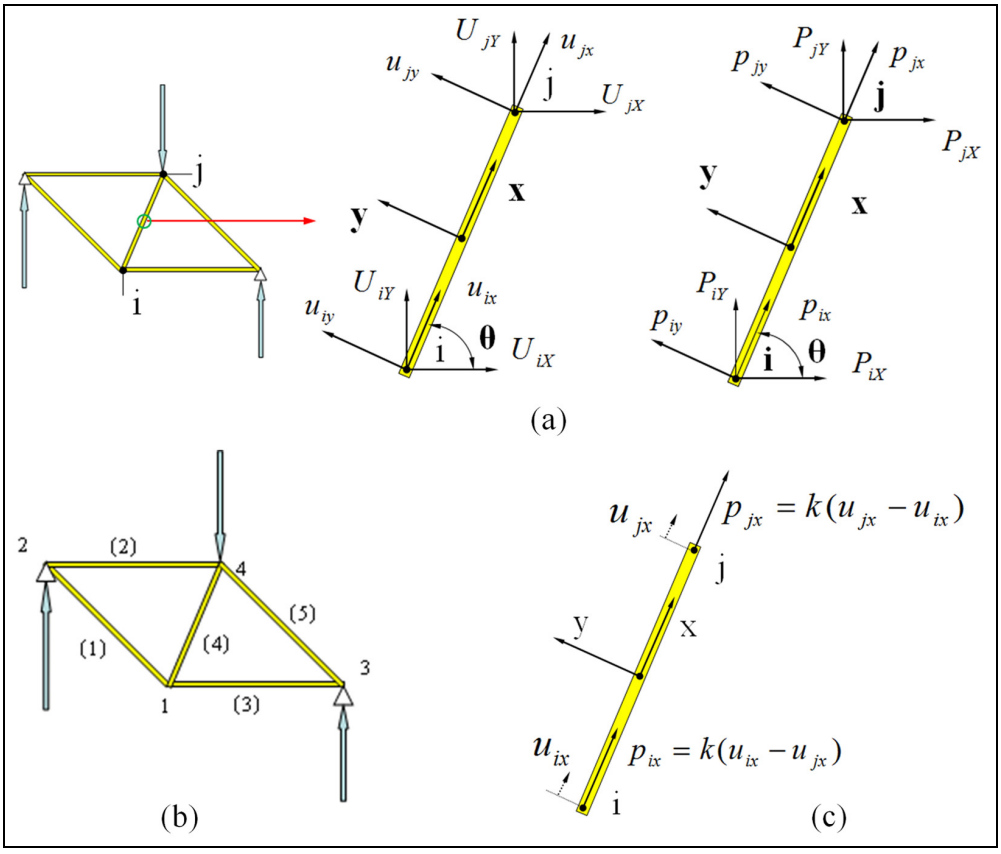

Figure 3. (a) Local and global displacement and force coordinates, (b) elements and nodes, and (c) structural forces on the bicycle frame.

Table 1. Relationships between each element and its corresponding node.

Element	Node *i*	Node *j*	θ
(1)	1	2	133.33
(2)	2	4	0
(3)	1	3	0
(4)	1	4	74
(5)	3	4	128.2

$$[K]^{(e)} = k \begin{bmatrix} \cos^2\theta & \sin\theta\cos\theta & -\cos^2\theta & -\sin\theta\cos\theta \\ \sin\theta\cos\theta & \sin^2\theta & -\sin\theta\cos\theta & -\sin^2\theta \\ -\cos^2\theta & -\sin\theta\cos\theta & \cos^2\theta & \sin\theta\cos\theta \\ -\sin\theta\cos\theta & -\sin^2\theta & \sin\theta\cos\theta & \sin^2\theta \end{bmatrix} \tag{5}$$

The stiffness matrix $[K]^{(e)}$ can be obtained from the previous derivation for a member element of the bicycle frame.

From the above results and the analysis of the stiffness matrix of the bicycle frame elements, the boundary conditions and load are set in order to obtain the normal stress on the tubes and the local and global displacements. The structural dimensions of the bicycle frame are shown in Figure 3(b).

The structural bicycle frame is divided into nodes and elements. Assuming an approximate solution for the elements, this study derives the equation of each and the combination of elements. The problem is divided into nodes and elements: Each frame tube can be considered as an element and each member of the joint as a node. The frame is formed from four nodes and five stationary elements. Table 1 shows the relationships between each element of the bicycle frame and its corresponding node.

The global displacement of the matrix can be obtained by solving the algebraic equations. The negative sign indicates a compressive deformation, that is, −980.2 N of compressive stress is generated on the seat tube and down tube. From the combination or sum of the individual elements of the matrix, the global stiffness matrix can be obtained as

$$[K]^{(G)} = [K]^{(1G)} + [K]^{(2G)} + [K]^{(3G)} + [K]^{(4G)} + [K]^{(5G)} \tag{6}$$

As shown in Figure 3(c), a negative sign is assumed to indicate a force in the opposite direction. It is estimated that the internal forces on each bike frame tube and the average normal stress. The internal forces on the tube are given by

$$p_{ix} = k(u_{ix} - u_{jx}), p_{jx} = k(u_{jx} - u_{ix}) \tag{7}$$

where

$$\{U\} = \{T\}\{u\} \qquad \{u\} = \{T\}^{-1}\{U\} \tag{8}$$

Element nodes u_{ix} and u_{jx} are the local coordinates of the displacement in the x- and y-directions. The global displacement is expressed by a conversion matrix applied to the local displacement. The normal stress is given by

$$\sigma = \frac{p}{A} = \frac{k(u_{ix} - u_{jx})}{A} = \frac{\frac{AE}{L}(u_{ix} - u_{jx})}{A} = E\left(\frac{u_{ix} - u_{jx}}{L}\right) \tag{9}$$

A p-mesh is created for the two-dimensional (2D) and three-dimensional (3D) geometric element models, as shown in Figure 4. K is derived using the global T and the local u and p are integrated, and boundary conditions and load are set, and the displacement is calculated with the same procedure for 2D analysis. Figure 5 shows the stress and displacement analysis, respectively, of a 3D truss. Figures 4(d) and 5 show the von Mises stress and displacement deformation behaviors. The bicycle frame sizes sketch of solid model geometry is as shown in Figure 6.

The FEM is a numerical procedure to solve mathematical equations by simulating to validate the derived equations. CAE was used for solid modeling of frame structures. In the case of 3D complex structures, the direct CAE modeling was used integrating with FEM analysis to generate the stress–strain results. The 2D analysis considered most of the time to simplify problems and to compute the solution easily, whereas the 3D analysis is the most accurate one because it represents the actual shape of the bicycle frame.

Stress analysis of the frame

The practical application of analytical and computational mechanics using a model that being simple is familiar and attractive.[12,13] There are two important aspects of structural analysis; the first is intensity and life evaluation of the structure; the second is structural optimization. The framework of this study is as follows: computer-aided design (CAD), CAE, simulation and testing using finite element analysis (FEA), sensitivity analysis for optimization design, and customized programming interface.

Increase in the weight on turning

The reaction force $R'_f{:}R'r = b{:}a, \because a > b, R'r > R'_f$ and the weight on the rear wheel is higher, as shown in Figure 7(a)

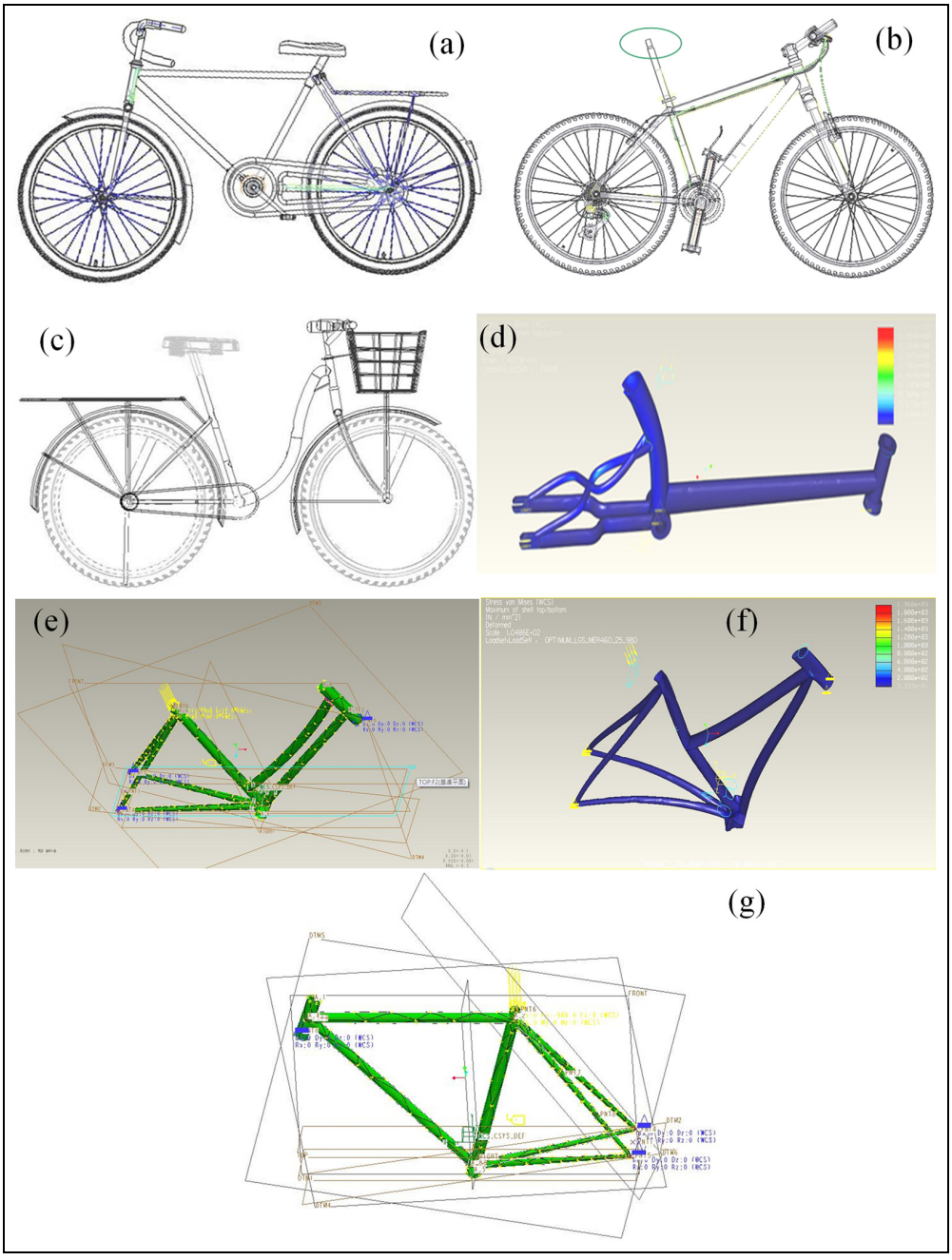

Figure 4. Analysis of a: (a) diamond, (b) mixte, (c) U, (d) H, (e) loop, (f) staggered types of bicycle frames, and (g) three-dimensional truss using fixed support and P mesh conditions.

$$\begin{aligned} \sum F_y &= R\cos\theta - W = 0 \\ R &= \frac{mg}{\cos\theta} \\ \sum F_x &= R\sin\theta = \frac{W}{g}a_x \\ \frac{W}{\cos\theta}\sin\theta &= \frac{W}{g}\frac{v^2}{\rho} \\ v^2 &= g\rho\tan\theta \end{aligned} \tag{10}$$

Increase in the weight on braking

The reaction force $R'_f{:}R'r = b{:}a, \because b > a, R'_f > R'r$ and the load on the front wheel is higher. As the brake load increases, when $a = 0$, the bicycle will fall forward, as shown in Figure 7(b).

Weight on the body when turning and braking

The reaction force R'' = body weight + R' (turn + brake). When only turning, the weight of the rear wheel

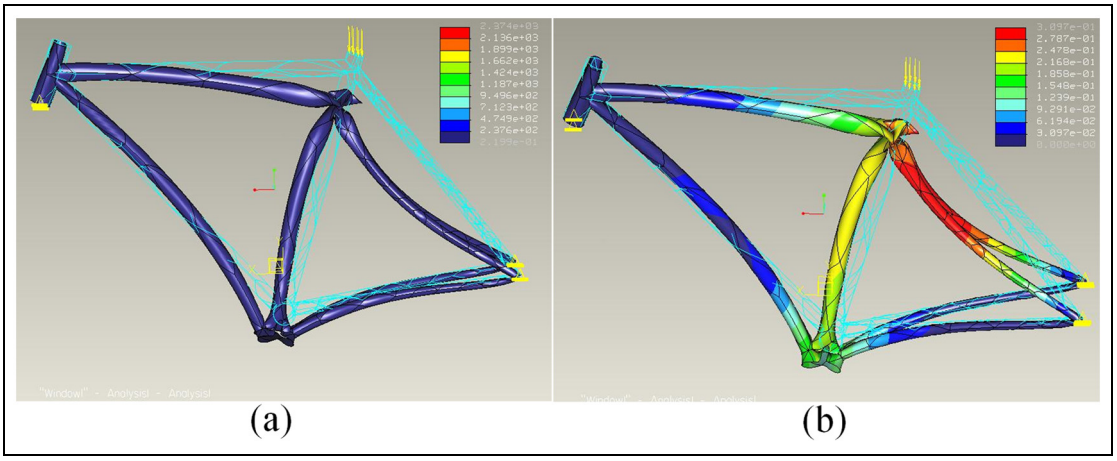

Figure 5. (a) Stress analysis and (b) displacement analysis of a bicycle frame.

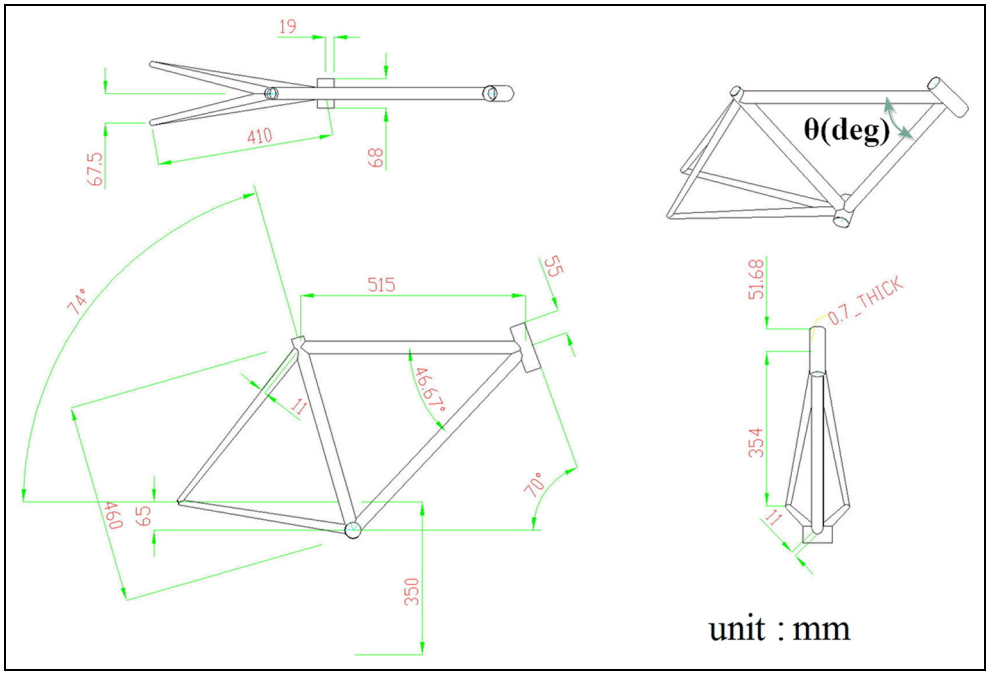

Figure 6. ProEngineer sketch of solid model geometry.

is higher. When only braking, the weight on the front wheel is higher. When both turning and braking, the load on the frame load is highest, as shown in Figure 7(c).

It is often assumed that the contact between a bicycle tire and the ground is frictionless. If the contact surface is frictionless, then a force on this surface will be perpendicular to the surface. If the ground is rough or undulating, then the tire will produce a tangential force to prevent relative movement between the tire and the ground, including rolling and sliding. Such resistance is called friction (friction force). This friction force has a certain limit; if the foot pedal or handle administers a sufficiently large force, it can prevent the movement.

From this structural analysis, the maximum static friction F_m with the vertical component of the surface reaction force is proportional to N, that is, $F_m = \mu_s N$, where μ_S is a constant and is called the static friction coefficient (or the coefficient of static friction). Similarly, the dynamic friction F_k of a bicycle also has the same form, that is, $F_k = \mu_k N$, where μ_k is a constant and is called the dynamic friction coefficient (or coefficient of kinetic friction). The friction coefficients μ_S and μ_k do not depend on the bicycle tires and the contact area with the ground but have a close relationship with the characteristics of the tires and the terrain. Turning (left side of Figure 7(d)) increases the load as a result of centripetal acceleration, while braking (right

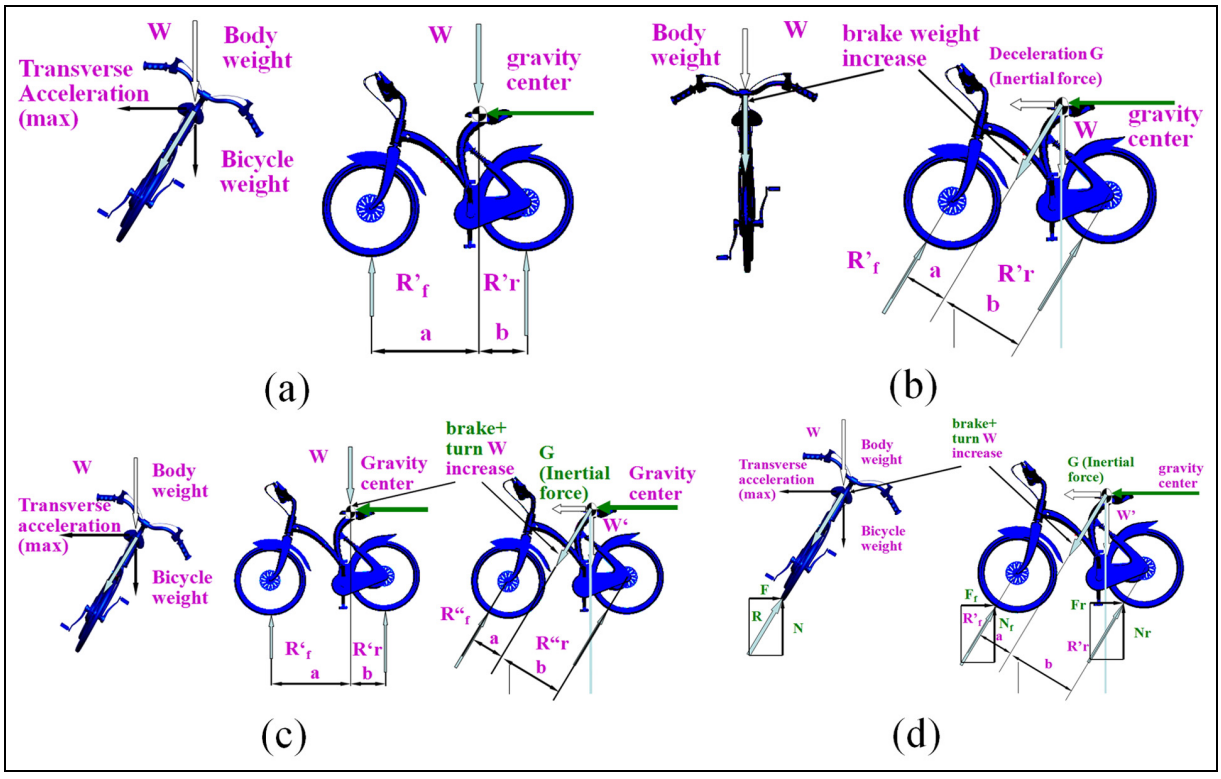

Figure 7. Analysis of the effect of: (a) external forces on a turning, (b) external forces on a braking, (c) external forces on the weight of a braking and turning, and (d) inertia and friction forces on the weight of a braking and turning bicycle.

Table 2. Deformation of the different materials bicycle frame in the present simulation compared with those in other studies.[14–17]

Notation	Specification	Yield strength (MPa)	Ultimate tensile strength (MPa)	Deformation (mm)	Reference
AZ61/BA	Extruded AZ61 Mg alloy before annealing	131.9 ± 1.2 (0)	310.9 ± 3.8 (0)	0.41–0.90	This study
AZ61 ECAE	Al_2O_3p Bc route 5%[14]	150.5	362.1	0.28–0.62	This study
Al6061-T6	Thermal treatment—hardening	260–290	300–320	0.27–0.59	This study
Mg alloy	Bicycle frame (pos. n.:8)	Type: YBM-R-MTB, mass: 1245 g, size: 19.5″/26″		0.071%–0.270%	Barna et al.[15]
Al6061-T6	Simulation of on-road bicycle frame	260–290	300–320	6.23–12.13	Cheng et al.[16]
Al6061-T6	Thermal treatment—hardening	260–290	300–320	4.1–4.7	Rontescu et al.[17]

side of Figure 7(d)) increases the load as a result of inertial force. The friction $F_k = \mu_k N$, as shown in Figure 7(d).

It is make the following assumptions:

1. Excluding the effects of air resistance;
2. Ignoring the force of inertia;
3. Considering only a static load on the frame of;
4. Assuming the materials are isotropic substances;
5. Ignoring the fact that welding the material weakens their strength and analyze the aluminum tubes in ideal conditions.

Strain–energy theories

The Pro/MECHANICA structural analysis in "max_stress_vm" is based on strain–energy theory. We used Al6061 aluminum alloy, AZ61 magnesium alloy, and AZ61/Al_2O_{3p} MMCs processed by ECAE as shown in Table 2.

This study examines the Al6061 aluminum alloy as the material for the bicycle frame. The metallic properties of ductile materials, the von Mises stress and strain analysis, and optimal design theory are used. The theoretical analysis is according to the fourth metal material yield strength (strain energy theory)

$$\sigma' = \left[\frac{(\sigma_1 - \sigma_2)^2 + (\sigma_2 - \sigma_3)^2 + (\sigma_1 - \sigma_3)^2}{2}\right]^{\frac{1}{2}} \quad (11)$$

where σ_1, σ_2, and σ_3 are the three axes of the principal stresses.

This study analyzed the "max_stress_vm," which indicates the maximum von Mises stress on the bicycle frame (MPa). If the requirements do not exceed the yield stress σ_y of the normal stress, then it can be written as the safety factor $F.S. = \sigma_Y/\sigma_{Mises}$, which has a yield strength 241 MPa and a tensile strength of 290 MPa of Al6061-T6 aluminum alloy.

Sensitivity analysis and optimized design

The main purpose analysis of local sensitivity is to discover an important parameter affecting stress on the bicycle frame

$$\text{Sensitivity} = \frac{\text{Structure response or mass change}}{\text{Changes in design parameters}}$$

For global sensitivity analysis, researchers implementing an optimized design must distinguish between what is most critical and the maximum and minimum values of the planning parameters.

The entire research also includes local and global sensitivity analysis to understand the impact of stress changes in the key parameters. The methodology consists first of establishing optimum dimensions for the frames. Optimization design goals are total mass minimize (weight lighter) and design limits von Mises stress (σ_e) < yield strength (Sy).

Results and discussion

It was observed that for a frame with the upper tube parallel to the down tube, the higher the tube center distance, the higher the intensity and the amount of deformation becomes smaller.

For a triangular-type frame (where the centerlines of the down tube and head tube intersect), its rigidity is higher than that of the loop-type frame (where the top tube is parallel to the down tube). In addition, for the upper tube and down tube of triangular frame, the higher the angle, the higher the rigidity. The upper level of the tube frame (diamond-type) reached maximum rigidity and minimum deformation, as shown in Figure 8.

This study attempts to verify the stress and displacement of several types of bicycle frames by applying a wireframe model and then analyze the solid structure. The maximum stress at the design limits is the von Mises stress. Conducting various bicycle frame thin shell entities, the top-down tube angle, top-down tube center distance, tube thickness, and top-down tube radius target parameters (goal) shows the maximum stress value (max_stress_vm), whereas the local and global sensitivity analysis results in optimum design of the total mass.

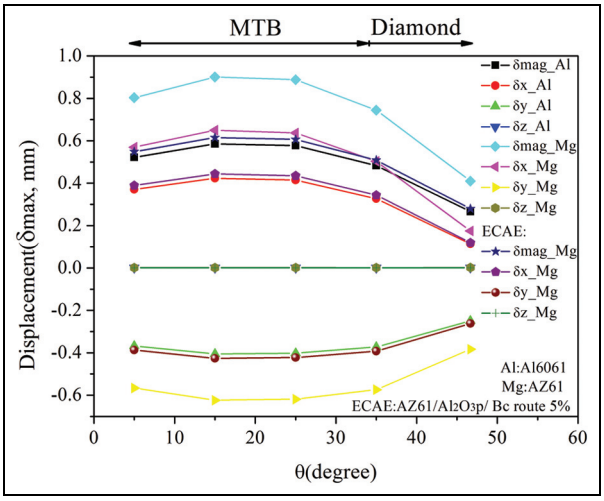

Figure 8. Effects of different angles on the stress and displacement of the bicycle frame.

The mechanical properties and deformation of the present simulation and other materials are listed in Table 2. The rigidity of the aluminum alloy is better than that of the magnesium alloy frame, and the rigidity of present studies of AZ61 MMCs with Al_2O3_p reinforced phase is improved by the ECAE process.

Obtained from the analyzed data, for a shell-entity frame, the diamond-type frame (diamond-shaped) has the highest rigidity, followed by the triangular frame (mixte and staggered shapes), then the parallel frame with larger pipe center distance, and finally, the parallel frame with smaller pipe center distance, which has the least rigid, as shown in Figures 9 and 10.

According to the simulation results, all of the amounts of deformation of the ECAEed AZ61/Al_2O_3 MMC bicycle frame are smaller than those of the magnesium alloy bicycle frame without adding Al_2O_3 as the reinforcement phase but are similar to those of aluminum alloy bicycle frame, as shown in Figure 11. Meanwhile, all of strain energies of the ECAEed AZ61/Al_2O_3 MMC bicycle frame are smaller than those of magnesium alloy bicycle frame without adding Al_2O_3 as the reinforcement phase but are similar to those of the aluminum alloy bicycle frame. Finally, all of the stresses of the ECAEed AZ61/Al_2O_3 MMC bicycle frame are smaller than those of the aluminum alloy bicycle frame. This indicates that ECAEed AZ61/Al_2O_3 MMCs has better yield stress than AZ61, which is similar to the yield stress of Al6061. In summary, ECAEed AZ61/Al_2O_3 MMCs almost achieve the level of Al6061 aluminum.

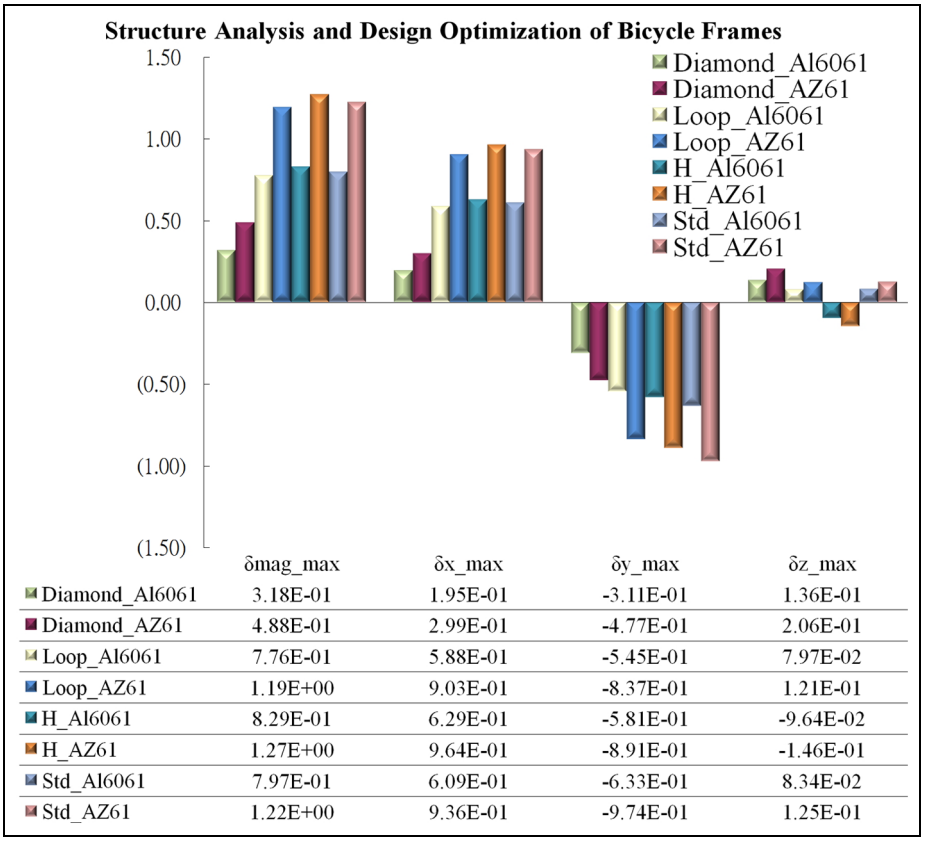

	δmag_max	δx_max	δy_max	δz_max
Diamond_Al6061	3.18E-01	1.95E-01	-3.11E-01	1.36E-01
Diamond_AZ61	4.88E-01	2.99E-01	-4.77E-01	2.06E-01
Loop_Al6061	7.76E-01	5.88E-01	-5.45E-01	7.97E-02
Loop_AZ61	1.19E+00	9.03E-01	-8.37E-01	1.21E-01
H_Al6061	8.29E-01	6.29E-01	-5.81E-01	-9.64E-02
H_AZ61	1.27E+00	9.64E-01	-8.91E-01	-1.46E-01
Std_Al6061	7.97E-01	6.09E-01	-6.33E-01	8.34E-02
Std_AZ61	1.22E+00	9.36E-01	-9.74E-01	1.25E-01

Figure 9. Effects on the maximum displacement of the different bicycle frame.

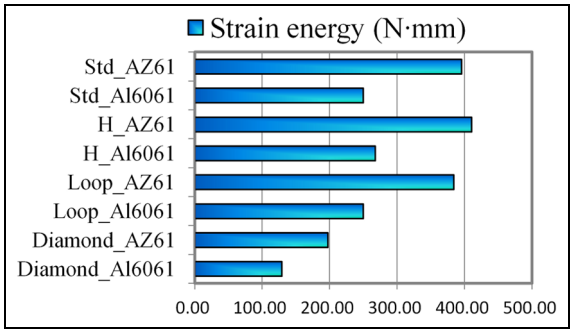

Figure 10. Effects on the strain energy of the different bicycle frame.

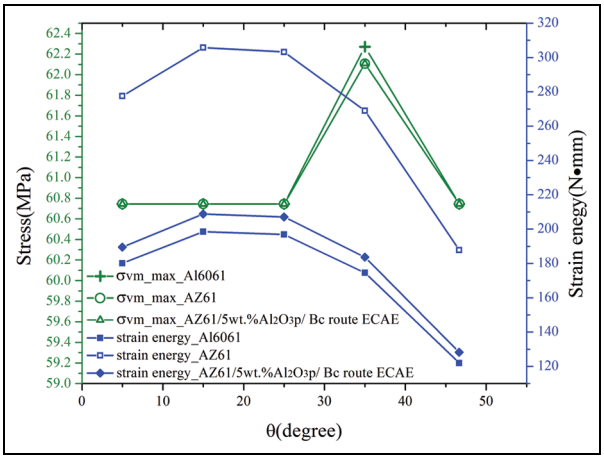

Figure 11. Effects of different angles on the stress and strain energy of the bicycle frame.

Conclusion

This article compares the maximum stress and displacement for different top-down tube center distances for the optimized design of a loop-type entity. From computer analysis of a loop-type wireframe, different center distances for the top-down tube did not significantly affect the seat tube displacement and strain energy. Yet, on the whole, the loop-type frame has a deformation larger than that of a frame in which the top-down tube has a higher angle. This is because in the wireframe analysis, in a parallel tube with similar characteristics for the four-bar linkage frame mechanism, the front and rear wheel center tubes place limits on its freedom (i.e. the whole frame is welded). The deformation node of the loop-type frame is more than that of the triangle frame, and its structure is less rigid. Finally, when the centerlines of the top tube and the down tube intersect with the head tube, the structure

has improved rigidity, so the amount of deformation decreases.

Through Pro/ENGINEER-MECHANICA, the results of digital solid modeling software CAE analysis show that all of the displacement, strain energy, and stress of the bicycle frame made of magnesium alloy materials without adding Al_2O_3 as the reinforcement phase are higher than those of the bicycle frame made of aluminum alloy.

For the mountain bike (MTB) frame simulated with ECAEed AZ61/Al_2O_3 MMCs, the calculation results show that not only is the rigidity similar to that of Al6061 but also compared to Al6061 aluminum alloy, the weight can be reduced from 4.0123 to 2.5764 kg (a weight reduction percentage of 36%). It is a bicycle frame of optimum size with lightweight in compliance with structural rigidity requirements.

Declaration of conflicting interests

The author(s) declared no potential conflicts of interest with respect to the research, authorship, and/or publication of this article.

Funding

The author(s) received no financial support for the research, authorship, and/or publication of this article.

References

1. Galvin P and Morkel A. Modularity on industry structure: the case of the world the effect of product bicycle industry. *Ind Innov* 2001; 8: 31–47.
2. Ninan JA and Siddique Z. Internet-based framework to support integration of the customer in the design of customizable products. *Proc IMechE, Part B: J Engineering Manufacture* 2007; 221: 529–538.
3. Siddique Z and Ninan JA. Modeling of modularity and scaling for integration of customer in design of engineer-to-order products. *Integr Comput-Aid E* 2006; 13: 133–148.
4. Schuijbroek J, Hampshire RC and van Hoeve W-J. Inventory rebalancing and vehicle routing in bike sharing systems. *Eur J Oper Res* 2017; 257: 992–1004.
5. Ricard MD, Hills-Meyer P, Miller MG, et al. The effects of bicycle frame geometry on muscle activation and power during a Wingate anaerobic test. *J Sport Sci Med* 2006; 5: 25–32.
6. Christiaans H and Bremner A. Comfort on bicycles and the validity of a commercial bicycle fitting system. *Appl Ergon* 1998; 29: 201–211.
7. Liu XJ, Wang JY, Yu WY, et al. Analysis and optimum design of rider-bicycle mechanisms: design of bicycle parameters for a specified rider. *Sci China Technol Sc* 2011; 54: 3027–3034.
8. Wilson DG and Papadopoulus J. *Bicycling science*. 3rd ed. London: The MIT Press, 2004, pp.312–315.
9. Huang SJ and Lin PC. Grain refinement of AM60/Al_2O_3p magnesium metal-matrix composites processed by ECAE. *Kovove Mater* 2013; 51: 357–366.
10. Huang SJ, Lin PC and Aoh JN. Mechanical behavior enhancement of AM60/Al_2O_3p magnesium metal–matrix nanocomposites by ECAE. *Mater Manuf Process 2015*; 30: 1272–1277.
11. Chang RR. Finite element analyses and experimental considerations of the deflection and failure behaviour of an asymmetric laminate composite bicycle handlebar. *Proc IMechE, Part E: J Process Mechanical Engineering* 2002; 216: 207–218.
12. Escalona JL and Recuero AM. A bicycle model for education in multibody dynamics and real-time interactive simulation. *Multibody Syst Dyn* 2012; 27: 383–402.
13. Klein RE. Using bicycles to teach system dynamics. *IEEE Contr Syst Mag* 1989; 9: 4–9.
14. Hsu ZW. *Effect of equal channel angular extrusion on the mechanical properties of AZ61 matrix composites with different reinforcement*. Master's Thesis, National Taiwan University of Science and Technology, Taipei, Taiwan, 2014.
15. Barna T, Bretz K, Fodor T, et al. Experimental testing of magnesium and chrome-molybdenum-alloy bicycle frames. *IEEE T Veh Technol* 2002; 51: 348–353.
16. Cheng YC, Lee CK and Tsai MT. Multi-objective optimization of an on-road bicycle frame by uniform design and compromise programming. *Adv Mech Eng* 2016; 8: 115.
17. Rontescu C, Cicic TD, Amza CG, et al. Choosing the optimum material for making a bicycle frame. *Metalurgija* 2015; 54: 679–682.